35th Annual International Conference of the IEEE EMBS
Osaka, Japan, 3 - 7 July, 2013

Estimation of Fiber Orientation by Filtered Q-ball Imaging*

Kuan-Hung Cho, Chun-Hung Yeh, Li-Wei Kuo, Yi-Ping Chao, and Ching-Po Lin

Abstract— **We proposed a filtered q-ball imaging (fQBI) method for the reconstruction of fiber orientation distribution function (ODF) together with the quantitative comparison to unfiltered QBI. The filter kernel increases the high angular frequency content that is beneficial for the angular resolution in resolving crossing fibers. Through a series of simulations using Monte-Carlo model, the angular resolution of fQBI was demonstrated better than traditional QBI but the deviation of fiber orientation estimate also becomes larger. The improvement of the angular resolution can also reduce the underestimation of separation angles as well as the bias of fiber orientation estimations. In conclusion, fQBI was demonstrated to improve the angular resolution of QBI in resolving crossing fibers. This improvement will be helpful to precisely reconstruct fiber tract and brain network in applications by QBI.**

I. Introduction

Diffusion magnetic resonance imaging (MRI) is a noninvasive imaging technique widely used in researches of brain disease, such as multiple sclerosis, trauma and brain tumor [1]. In the last decade, the technical development of white matter tracts reconstruction using diffusion MRI resulted in increasing applications to investigate the structural connectivity of the brain. Diffusion tensor imaging (DTI) firstly mapped intravoxel fiber population by modeling three-dimensional diffusion profile as a tensor [2]. Because of well-known limitations of DTI in regions containing multiple fiber populations [3, 4], several works have attempted to overcome the deficient of DTI model with high angular resolution diffusion image (HARDI) acquisition [5] by either improving model of multiple fiber crossings [5-7] or generalizing the analysis of probability distribution of water diffusion [8-11].

Q-ball imaging (QBI), one of the model-free methods, obtains the orientation distribution function of water molecular diffusion by applying Funk-Radon transform (FRT) to HARDI acquisition and have been validated its ability to solving intravoxel fiber crossings [9, 12]. However, the blurring effect from the radial integral of FRT makes QBI failure in distinguishing fiber crossings with small separation angles [13]. Hess et al. reformulated the q-ball reconstruction in terms of spherical harmonic basis functions, which yielded an analytic solution with useful properties of a frequency domain representation [14]. The representation in frequency domain helps us to process on the frequency components according to our purpose. In this article, we proposed a filtered QBI (fQBI) reconstruction to increase the angular resolution of QBI in solving fiber crossings by enhancing high angular frequency components. Quantitative comparisons between QBI and fQBI were performed using Monte-Carlo simulations. The simulation results showed that fQBI can distinguish two fiber crossings in the cases of low b value or small separation angles while single fiber is predicted by QBI. Although QBI can also resolve two fiber crossings in some cases, obvious biases of fiber orientation estimate as well as underestimate of separation angle can be observed due to insufficient angular resolution, which is improved in fQBI reconstruction. The simulations demonstrate that the angular resolution of QBI is increased by increasing the power of high angular frequency components using a high pass filter. In the meanwhile, the fiber orientations in voxels containing two fiber crossings can be estimate more accurately by fQBI, which is able to provide brain connectivity more correctly.

*Research supported by ME-102-PP-06 and NSC 101-2218-E-182 -005.

K.-H. Cho, C.-H. Yeh, and C.-P. Lin† are with the Institute of Neuroscience, National Yang-Ming University, Taipei, Taiwan (e-mail (Cho): kh.michael.cho@gmail.com; e-mail (Yeh): jimmy.chyeh@gmail.com; e-mail (Lin): cplin@ym.edu.tw; phone: 886-2-28267338; fax: 886-2-28262285).

Li-Wei Kuo is with the Division of Medical Engineering Research, National Health Research Institutes, Miaoli County, Taiwan (e-mail: lwkuo@nhri.org.tw).

Yi-Ping Chao is with the Department of Computer Science and Information Engineering, Chang Gung University, Tao-Yuan, Taiwan (e-mail: yiping@mail.cgu.edu.tw).

II. Materials and Methods

A. QBI reconstruction with high pass filter

QBI was proposed to estimate the ODF by applying FRT on HARDI acquisition, which is defined as [9]

$$ODF_{q_0}(\mathbf{u}) = \int S(\mathbf{q})\delta(\mathbf{q}\cdot\mathbf{u})\delta(|\mathbf{q}| - q_0)d\mathbf{q}, \qquad (1)$$

where $\mathbf{u}$ is the unit vector of direction of interest and $S(\mathbf{q})$ represents the diffusion signal measured with gradient wave vector $\mathbf{q}$. $\delta(\bullet)$ represents the Dirac delta function and q_0 means that diffusion signals are sampled on the shell with $|\mathbf{q}|=q_0$. A spherical radial basis function (sRBF) was used to interpolate signals on the set of points perpendicular to $\mathbf{u}$ for the implementation of (1) [9]. Equation (1) can be reformulated with spherical harmonics basis function [14].

$$ODF_{q_0}(\mathbf{u}) = \sum_{l}^{L}\sum_{m=-l}^{l} 2\pi P_l(0) c_l^m Y_l^m(\mathbf{u}), \qquad (2)$$

where $P_l(\mathrm{x})$ denotes the unassociated Legendre polynomial of order l, c_l^m denote the harmonic series coefficients, $Y_l^m(\mathrm{u})$ is the spherical harmonics and L is the harmonic series order. Because spherical harmonic expansion of a function represents the generalization of the Fourier transform on the sphere, we can easily filter the signal by adjusting the weight

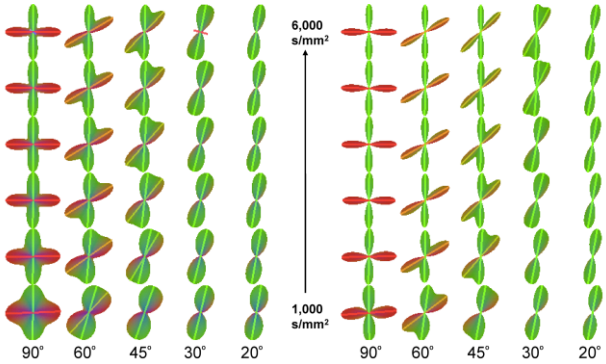

Figure 1. ODFs estimated from high SNR data (SNR=100) by unfiltered (a) and filtered (b) QBI with b values from 1,000 s/mm^2 to 6,000 s/mm^2 and separation angles at 20^o to 90^o.

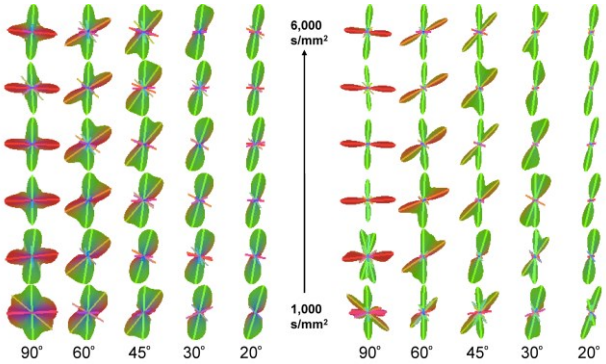

Figure 2. ODFs estimated from low SNR data (SNR=10) by unfiltered (a) and filtered (b) QBI with b values from 1,000 s/mm^2 to 6,000 s/mm^2 and separation angles at 20^o to 90^o.

of the harmonic series coefficients by introducing a kernel $h(l)$, and (2) can be modified as

$$ODF_{q_0}(\mathbf{u}) = \sum_{l}^{L} \sum_{m=-l}^{l} 2\pi P_l(0) h(l) c_l^m Y_l^m(\mathbf{u}), \qquad (3)$$

To increase the angular resolution of QBI, the kernel $h(l)$ was chosen as

$$h(l) = kl, \qquad (4)$$

where k controls the slope of $h(l)$ and is chosen as 0.5 here. With (4), the high frequency harmonics can be enhanced and the angular resolution of QBI could be improved.

B. Numerical Simulations

To investigate the accuracy and the angular resolution for filtered and unfiltered QBI, numerical simulations were performed using three-dimensional Monte Carlo simulations of diffusion, where water molecules were considered as random walkers. The neuronal fiber was modeled as a single impermeable cylinder. Total reflection rule was used to model the collision of water molecules with the surface of cylinder. Two fiber populations with orientations separated by a prescribed angle were placed on x-y plane to simulate intravoxel two fiber crossings. The diffusion signal attenuation was then calculated based on pulsed-gradient spin-echo experiment [15, 16]. By reference to parameter settings of clinical scanners, the diffusion time and gradient duration were set to 50 and 40 ms and 80 non-collinear gradient directions equally distributed on hemisphere were encoded. Six b values, from 1,000 to 6,000 s/mm^2 in an increment of 1,000 s/mm^2, were investigated and the gradient strength was adjusted according to the b value. Five separation angles (20^o, 30^o, 45^o, 60^o, and 90^o) were used for the investigation of the angular resolution of filtered and unfiltered QBI in estimating fiber crossings. Two SNR levels (100 and 10) were used to investigate the accuracy of fQBI under different noise level. Noisy diffusion signals were created by adding Gaussian noise (mean=0 and standard deviation=$S(0)$/SNR) to both real and image part of noiseless complex diffusion signals. For each SNR level, the analysis was repeated for 100 times to study the deviation of fiber orientation estimates by fQBI and QBI.

C. Fiber Orientation Reconstruction

The implementation of QBI reconstruction is based on the procedure proposed by Hess et al. [14] and the implementation of fQBI reconstruction is modified by adding filter kernel $h(l)$ to QBI reconstruction. Therefore, all reconstruction parameters were kept the same for both QBI and fQBI reconstruction. The harmonic series order L was set to be 10, which needs at least 61 diffusion measurements to calculate the harmonic coefficients. The obtained ODFs were sampled on 642 directions generated from an eight-fold tessellated icosahedrons, offering an angular sampling resolution of around 8^o. The fiber orientations were defined the directions of local maxima of the reconstructed ODF. These directions were then set as an initial simplex for searching the local maxima using Nelder-Mead method in

TABLE I. ESTIMATED SEPARATION ANGLES WITH HIGH SNR

b value (s/mm^2)	Prescribed separation angles (degree)				
	90	*60*	*45*	*30*	*20*
1,000	86.53±1.78	29.72±5.05	-	-	-
	83.88±2.84	48.11±4.46	27.06±3.94	-	-
2,000	88.69±0.64	50.06±0.81	20.20±1.83	-	-
	87.77±1.13	58.25±1.20	37.90±1.00	-	-
3,000	89.22±0.42	55.20±0.46	32.26±0.81	-	-
	88.82±0.66	59.51±0.66	42.58±0.57	-	-
4,000	89.56±0.30	57.16±0.39	37.74±0.38	87.30±1.63	-
	89.38±0.42	59.97±0.51	44.16±0.40	12.85±7.91	-
5,000	89.68±0.22	58.07±0.30	40.26±0.26	81.05±23.90	88.96±0.00
	89.58±0.30	60.18±0.41	44.68±0.25	21.83±1.41	-
6,000	89.77±0.18	58.63±0.25	41.49±0.20	86.04±9.71	-
	89.71±0.23	60.43±0.32	44.78±0.20	25.80±0.68	-

TABLE II. ESTIMATED SEPARATION ANGLES WITH LOW SNR

b value (s/mm^2)	Prescribed separation angles (degree)				
	90	*60*	*45*	*30*	*20*
1,000	68.82+21.49	42.79+17.01	53.27+25.37	62.98+25.69	73.10+18.49
	64.49+20.51	44.46+15.14	38.07+9.55	34.95+10.31	34.93+11.45
2,000	82.59+9.41	47.96+9.65	49.57+27.58	72.40+18.91	75.47+10.70
	76.79+15.83	56.59+10.56	39.87+12.31	47.96+21.54	57.70+22.90
3,000	86.37+2.66	55.32+4.38	44.60+17.95	71.64+12.99	72.48+15.91
	84.69+3.99	60.17+6.66	42.92+7.78	56.50+23.81	67.87+14.62
4,000	87.24+2.11	56.42+3.36	39.37+7.33	67.47+19.68	70.30+13.16
	86.10+3.01	58.90+4.77	43.19+3.23	52.69+23.00	66.38+15.72
5,000	87.59+1.66	58.19+2.77	38.96+2.81	67.24+17.50	66.08+18.82
	86.96+2.07	60.43+3.44	43.05+2.27	52.54+24.50	66.82+14.89
6,000	87.56+1.57	58.20+2.34	40.67+2.27	58.74+24.59	66.07+15.16
	87.07+2.01	59.88+2.88	43.47+1.95	42.34+22.85	64.52+15.35

TABLE III. ESTIMATED FIBER ORIENTATIONS WITH HIGH SNR

b value (s/mm^2)	Prescribed separation angles (degree)				
	90	*60*	*45*	*30*	*20*
1,000	1.77±0.97	14.99±4.86	-	-	-
	3.53±1.74	6.09±1.67	10.06±1.70	-	-
2,000	0.66±0.37	5.21±0.58	12.43±1.28	-	-
	1.28±0.70	1.55±0.68	4.16±1.03	-	-
3,000	0.49±0.27	2.60±0.31	6.66±0.53	-	-
	0.80±0.44	0.65±0.36	1.68±0.49	-	-
4,000	0.31±0.20	1.61±0.25	3.89±0.29	14.63±0.83	-
	0.47±0.29	0.34±0.26	0.77±0.31	6.51±0.82	-
5,000	0.33±0.18	1.16±0.21	2.58±0.22	14.58±1.31	9.62±0.00
	0.47±0.25	0.27±0.22	0.45±0.22	4.27±0.70	-
6,000	0.31±0.15	0.92±0.16	1.94±0.18	14.37±2.95	-
	0.41±0.19	0.29±0.21	0.39±0.18	2.28±0.40	-

TABLE IV. ESTIMATED FIBER ORIENTATIONS WITH LOW SNR

b value (s/mm^2)	Prescribed separation angles (degree)				
	90	*60*	*45*	*30*	*20*
1,000	2.66±19.17	14.47±11.26	15.22±8.94	12.62±6.24	10.44±4.18
	5.58±22.23	10.04±12.91	8.35±8.58	5.72±5.44	6.08±5.10
2,000	0.91±3.78	7.25±8.38	15.08±10.43	14.82±4.47	10.20±2.81
	0.56±9.59	2.49±5.01	5.68±8.10	10.41±6.88	9.93±4.65
3,000	0.07±1.84	2.72±2.59	10.81±11.31	14.63±4.23	10.09±1.99
	0.37±2.83	1.00±3.49	3.11±6.01	11.07±7.33	10.29±3.52
4,000	1.02±1.37	1.77±2.12	4.57±4.17	14.84±5.17	10.17±1.73
	1.27±2.21	0.60±2.48	1.59±2.35	10.64±8.24	10.17±3.00
5,000	0.32±1.52	1.14±1.31	3.10±2.09	14.08±6.12	9.59±1.55
	0.26±2.17	0.28±1.70	1.14±1.76	9.39±9.07	9.42±2.48
6,000	0.49±1.27	1.22±1.16	2.20±1.22	14.14±7.16	9.55±1.45
	0.68±1.54	0.46±1.56	0.94±1.25	7.01±8.59	9.28±2.13

order to reduce the digitized error from ODF sampling. Because it is possibly to generate more than two fiber orientations due to the noise, the fiber orientations corresponding to the two largest ODF values were selected and classified according to the separation angle between estimated fiber orientation and the orientation of prescribed fiber population. All reconstruction were implemented by home-made codes using MATLAB (The MathWorks, Inc., USA).

I. RESULTS

Fig. 1 shows the ODFs reconstruction from high SNR data (SNR=100) by QBI (left) and fQBI (right). The estimated fiber orientation is indicated by line. It can be observed that the lobes of ODF by fQBI are more sharpening than that by QBI, which helps to distinguish fiber crossings with small separation angles at low b value. The ODF reconstructed from low SNR data (SNR=10) are shown in Fig. 2. At low SNR, fake fibers can be observed in ODFs by QBI while fQBI enhances these fake fibers. Table I lists the separation angles estimated from high SNR data by QBI (white) and fQBI (grey). The results of estimated separation angles from low SNR data are listed in Table II. The estimated separation angles are presented as mean ± standard deviation (STD), and hyphen means single fiber is detected by QBI or fQBI. It can be observed that the STD of separation angle estimated by fQBI is slightly greater than QBI in the cases that the angular resolution is sufficient, e.g. the cases for 90^o prescribed separation angle. In the cases for 45^o prescribed separation angle, the mean separation angles from fQBI are more close to the 45^o than that from QBI, which implies that higher angular resolution can be achieved by fQBI reconstruction. Table III showed the fiber orientation estimate of the fiber population on y axis by QBI and fQBI with high SNR data, and Table IV listed the results with low SNR data. In Table III and IV, the results are presented as mean deviation angle ± STD. The mean deviation angle becomes larger with lower b value or smaller prescribed separation angle. This result agrees with the underestimate of the separation angles observed in Table I and II.

II. DISCUSSIONS

By simulating intravoxel fiber crossing using Monte-Carlo model, we tested the ability to resolve fiber crossings of QBI and fQBI respectively. The results showed that fQBI can resolve small separation angle than QBI at the same b value. The angular resolution could be improved by introducing high pass filtering in fQBI reconstruction comparing to QBI. On the contrary, QBI with low |q| values could not resolve fibers with small separation angles and resulted in the vague estimation of fiber orientations.We further observed the separation angle was underestimated and resulted in the vague estimation of fiber orientations even if QBI or fQBI successed to distinguish a fiber crossing. However, this phenomenon is more severe for QBI. Although fQBI showed higher ability to resolving fiber crossings than QBI, the estimation of fiber orientation by fQBI is prone to deviated from the true fiber orientation than QBI due to high sensitivity to noise in fQBI reconstruction.

A. Angular resolution in resolving fiber crossings

It was found that the angular resolution of QBI could be improved by increasing the encoded b value [17], which was also observed in our simulation results for QBI and fQBI. Since high frequency content increases with b value, increasing b value can result in similar results from high pass filtering. Therefore, fQBI is able to achieve the same angular resolution as QBI with lower b value, which helps to reduce echo time under a clinical MR system, whose gradient strength is limited.

Several studies tried to push the angular resolution of resolving fiber crossing to the limit by either deconvolution [18, 19] or ODF sharpening methods [20]. Our method is similar to latter method except the filter kernel is different. In [20], the kernel derived from Laplace-Beltrami operator is a nonlinear function $l^2(l+1)^2$. The kernel greatly increases the power of high angular resolution component comparing to the kernel used in this study, and is probably able to achieve higher angular resolution of fQBI. However, the noise will be amplified when increasing high frequency content by the filter, and results in large deviation of fiber orientation estimation comparing to unfiltered QBI. Therefore, there is a trade-off between the accuracy of fiber detection and the angular resolution when choosing the filter kernel. In this article, the filtered kernel chosen as $h(l)=l/2$ by considering both of the accuracy and the angular resolution. The filter kernel needs to be optimized for the trade-off between the accuracy and the angular resolution.

Previous studies showed that the angular resolution increased with harmonic order for methods that employ spherical harmonic basis [14, 21]. Fiber orientation reconstruction with higher harmonic series order involves higher frequency content which increases the angular resolution. However, the available harmonic series order is limited by the number of gradient directions for data acquisition. In this article, the HARDI data were generated with 80 gradient directions, which allow a maximum harmonic series order of 10 for numerical stability. By the use of filter kernel, fQBI achieved higher angular resolution with the same harmonic series order to avoid the numerical instability.

B. The accuracy for fiber orientation estimate

In Table I and II, it can be observed that the separation angle is greatly underestimated by QBI at low b value or with small prescribed separation angle, which was also seen in [17]. However, the underestimate of separation angle is mild for fQBI due to the better angular resolution. The average fiber orientation from 100 iterations tends to deviation from the true fiber orientation with lower b value or smaller prescribed separation angle, which is probably because of the insufficient angular resolution for resolving fiber crossing. A higher harmonic series order is probable to further improve the underestimation of separation angle. The harmonic series order of 10 used in this study was the maximum value under 80 encoded gradient directions. Another approach is to use other filter kernels that increase more high frequency content [20] or to use higher harmonic series order by super-resolution technique [21].

The STD listed in Table III and IV represents how the fiber orientation estimation fluctuated by noise. We could observe that the variation of fiber orientation estimation from QBI is always greater than QBI. Since lower harmonic series order removed the fluctuations in the data due to noise because of incapability of representing the high frequency spikes introduced by measurement noise, the variation can be reduced by using lower harmonic series order, which will slightly reduce the angular resolution. Therefore, a optimization work is needed for optimizing the reconsturciton of fQBI by considering both the accuracy and the angular resolution.

REFERENCES

[1] P. C. Sundgren, Q. Dong, D. Gomez-Hassan, S. K. Mukherji, P. Maly, and R. Welsh, "Diffusion tensor imaging of the brain: review of clinical applications," *Neuroradiology,* vol. 46, pp. 339-50, May 2004.

[2] P. J. Basser, J. Mattiello, and D. LeBihan, "MR diffusion tensor spectroscopy and imaging," *Biophysical journal,* vol. 66, pp. 259-267, 1994.

[3] A. L. Alexander, K. M. Hasan, M. Lazar, J. S. Tsuruda, and D. L. Parker, "Analysis of partial volume effects in diffusion-tensor MRI," *Magnetic Resonance in Medicine,* vol. 45, pp. 770-780, 2001.

[4] M. R. Wiegell, H. B. Larsson, and V. J. Wedeen, "Fiber crossing in human brain depicted with diffusion tensor MR imaging," *Radiology,* vol. 217, pp. 897-903, Dec 2000

[5] D. S. Tuch, T. G. Reese, M. R. Wiegell, N. Makris, J. W. Belliveau, and V. J. Wedeen, "High angular resolution diffusion imaging reveals intravoxel white matter fiber heterogeneity," *Magn Reson Med,* vol. 48, pp. 577-82, Oct 2002.

[6] Y. Assaf, R. Z. Freidlin, G. K. Rohde, and P. J. Basser, "New modeling and experimental framework to characterize hindered and restricted water diffusion in brain white matter," *Magn Reson Med,* vol. 52, pp. 965-78, Nov 2004.

[7] Y. Assaf, R. Z. Freidlin, G. K. Rohde, and P. J. Basser, "New modeling and experimental framework to characterize hindered and restricted water diffusion in brain white matter," *Magn Reson Med,* vol. 52, pp. 965-78, Nov 2004.

[8] J. D. Tournier, F. Calamante, D. G. Gadian, and A. Connelly, "Direct estimation of the fiber orientation density function from diffusion-weighted MRI data using spherical deconvolution," *Neuroimage,* vol. 23, pp. 1176-85, Nov 2004.

[9] D. S. Tuch, "Q-ball imaging," *Magn Reson Med,* vol. 52, pp. 1358-72, Dec 2004.

[10] V. J. Wedeen, P. Hagmann, W. Y. Tseng, T. G. Reese, and R. M. Weisskoff, "Mapping complex tissue architecture with diffusion spectrum magnetic resonance imaging," *Magn Reson Med,* vol. 54, pp. 1377-86, Dec 2005.

[11] F. C. Yeh, V. J. Wedeen, and W. Y. Tseng, "Generalized q-sampling imaging," *IEEE Trans Med Imaging,* vol. 29, pp. 1626-35, Sep 2010.

[12] M. Perrin, C. Poupon, B. Rieul, P. Leroux, A. Constantinesco, J.-F. Mangin, and D. LeBihan, "Validation of q-ball imaging with a diffusion fibre-crossing phantom on a clinical scanner." vol. 360, 2005, pp. 881-891.

[13] K. H. Cho, C. H. Yeh, J. D. Tournier, Y. P. Chao, J. H. Chen, and C. P. Lin, "Evaluation of the accuracy and angular resolution of q-ball imaging," *Neuroimage,* vol. 42, pp. 262-71, Aug 1 2008.

[14] C. P. Hess, P. Mukherjee, E. T. Han, D. Xu, and D. B. Vigneron, "Q-ball reconstruction of multimodal fiber orientations using the spherical harmonic basis," *Magn Reson Med,* vol. 56, pp. 104-17, Jul 2006.

[15] E. O. Stejskal, "Use of Spin Echoes in a Pulsed Magnetic-Field Gradient to Study Anisotropic, Restricted Diffusion and Flow," *The Journal of Chemical Physics,* vol. 43, pp. 3597-3603, 1965.

[16] E. O. Stejskal and J. E. Tanner, "Spin Diffusion Measurements: Spin Echoes in the Presence of a Time-Dependent Field Gradient," *The Journal of Chemical Physics,* vol. 42, pp. 288-292, 1965.

[17] K. H. Cho, C. H. Yeh, J. D. Tournier, Y. P. Chao, J. H. Chen, and C. P. Lin, "Evaluation of the accuracy and angular resolution of q-ball imaging," *Neuroimage,* vol. 42, pp. 262-71, Aug 1 2008.

[18] F. C. Yeh, V. J. Wedeen, and W. Y. Tseng, "Estimation of fiber orientation and spin density distribution by diffusion deconvolution," *Neuroimage,* vol. 55, pp. 1054-62, Apr 1 2011.

[19] M. Descoteaux, R. Deriche, T. R. Knosche, and A. Anwander, "Deterministic and Probabilistic Tractography Based on Complex Fibre Orientation Distributions," *Medical Imaging, IEEE Transactions on,* vol. 28, pp. 269-286, 2009.

[20] M. Descoteaux, E. Angelino, S. Fitzgibbons, and R. Deriche, "Regularized, fast, and robust analytical Q-ball imaging," *Magn Reson Med,* vol. 58, pp. 497-510, Sep 2007.

[21] J. D. Tournier, F. Calamante, and A. Connelly, "Robust determination of the fibre orientation distribution in diffusion MRI: Non-negativity constrained super-resolved spherical deconvolution," *NeuroImage,* vol. 35, pp. 1459-1472, 2007.